



## Design, Synthesis, Molecular Docking Studies and *in Silico* Prediction of ADME Properties of New 5-Nitrobenzimidazole/thiopyrimidine Hybrids as Anti-angiogenic Agents Targeting Hepatocellular Carcinoma

Heba T. Abdel-Mohsen<sup>a,\*</sup> and Ahmed M. El Kerdawy<sup>b,c</sup>



<sup>a</sup> Chemistry of Natural and Microbial Products Department, Pharmaceutical and Drug Industries Research Institute, National Research Centre, Dokki, Giza 12622, Egypt.

<sup>b</sup> Department of Pharmaceutical Chemistry, Faculty of Pharmacy, Cairo University, Kasr El-Aini Street, P.O. Box 11562, Cairo, Egypt.

<sup>c</sup> Department of Chemistry, School of Pharmacy, Newgiza University (NGU), Newgiza, km 22 Cairo-Alexandria Desert Road, Cairo, Egypt.

### Abstract

In the current study, a new series of 5-nitrobenzimidazole-pyrimidine hybrids **12a,b**, **13** and **14a-c** were designed as VEGFR-2 inhibitors targeting hepatocellular carcinoma. The designed and synthesized conjugates demonstrated a moderate to potent inhibitory activity on VEGFR-2 with IC<sub>50</sub> reaching 2.83 μM. Moreover, they demonstrated a moderate to potent cytotoxic activity on HepG2 cell line. Compound **14c** was the most potent hybrid with IC<sub>50</sub> of 2.83 μM on VEGFR-2 and IC<sub>50</sub> of 4.37 μM on HepG2 cell line. *In silico* docking of the synthesized hybrids **12a,b**, **13** and **14a-c** in the VEGFR-2 binding pocket proved their capability to perform the important interactions required for VEGFR-2 inhibition at its binding site. In addition, the synthesized molecules proved promising predicted ADME properties to be further optimized for the discovery of new targeted anticancer agents.

Keywords: Nitrobenzimidazole-thiopyrimidine; VEGFR-2; hepatocellular carcinoma; ADME.

### 1. Introduction

Hepatocellular carcinoma (HCC) is the most abundant form of liver malignancy and is one of the main types of cancer-related mortality around the world [1]. In this regard, pathological angiogenesis plays a significant role in the growth and proliferation of HCC [2-4]. For the cancer cells to grow, proliferate and move from one place to another (metastasis) a good blood supply is required to supply tumor cells with the essential nutrient, oxygen and to remove waste products [5]. One of the most important mechanisms adopted by the cancer cells is the up-regulation of a protein called vascular endothelial growth factor (VEGF) that binds to vascular endothelial growth factor receptors (VEGFR 1-3) on endothelial cells lining the tumor blood vessels walls resulting in growth and survival of new blood vessels [6, 7]. Drugs that target the angiogenesis are unique promising targeted anticancer agents that block the formation of new

blood vessels that support the tumor rather than acting directly on cancer cells [8]. One of the most successful strategies in developing anti-angiogenic agents is to use small molecules inhibitors that directly block the VEGFR-2. Recently, the USA food and drug administration (FDA) approved the prescription of different VEGFR-2 inhibitors for patients diagnosed with hepatocellular cancer [9]. Sorafenib (**I**) (Fig. 1) is the first multi-targeted protein kinase inhibitor which proved clinical effectiveness in the treatment of different HCC [10, 11]. Although, sorafenib (**I**) displayed an initial success, its positive effect was found to last for a short period and a rapid development of resistance was noticed by cancer cells [12, 13]. Recently, FDA approved the application of the multi-kinase inhibitors regorafenib (**II**) and lenvatenib (**III**) (Fig. 1) for the treatment of HCC [14-16]. However, the quick emergent resistance due to target proteins' mutations dictates the need for the discovery of new scaffolds that may act as anticancer alternatives.

1

\*Corresponding author e-mail: [ht.abdel-mohsen@nrc.sci.eg](mailto:ht.abdel-mohsen@nrc.sci.eg); [hebabdelmohsen@gmail.com](mailto:hebabdelmohsen@gmail.com); (Heba T. Abdel-Mohsen).

Received Date: 20 May 2023, Revised Date: 28 June 2023, Accepted Date: 16 July 2023

DOI: 10.21608/ejchem.2023.212212.7998

©2024 National Information and Documentation Center (NIDOC)

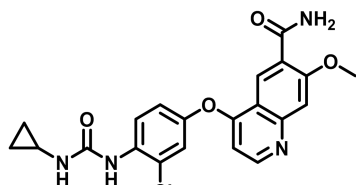
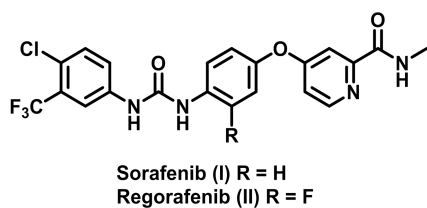


Fig. 1. FDA approved protein kinase inhibitors I-III

Lenvatinib (III)

Benzimidazole is a structural isostere of naturally occurring nucleotides, accordingly, it is broadly incorporated as a privileged scaffold in drug discovery [17]. Multiple benzimidazole derivatives were reported to have promising chemotherapeutic activity [18, 19]. In addition, different studies demonstrated the promising protein kinase inhibitory activity and specifically the anti-angiogenic activity of various benzimidazoles [20]. For instance, we have recently reported the discovery of novel 2-substituted benzimidazoles as potent VEGFR-2 inhibitors targeting breast cancer and hepatocellular carcinoma [21, 22]. Compounds IV and V (Fig. 2) are representative examples of the synthesized series and they revealed an  $IC_{50}$  of 1.26 and 0.11  $\mu$ M against VEGFR-2, respectively. In addition, compound IV displayed an  $IC_{50}$  of 22.58 and 21.25  $\mu$ M on HepG2 and MCF-7 cell lines, respectively, whereas derivative V displayed an  $IC_{50}$  of 1.98  $\mu$ M on HepG2 cell line [21, 22].

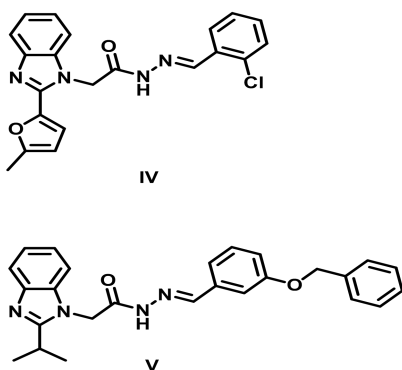
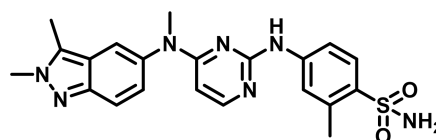
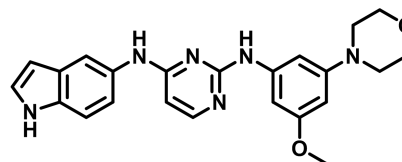


Fig. 2. The benzimidazole derivatives IV and V as VEGFR-2 inhibitors

In the meantime, pyrimidines and fused pyrimidines are interesting scaffold of diverse applications in different drugs [23-28]. Pazobanib (VI) and MKP116 (VII) (Fig. 3) are protein kinase inhibitors that incorporate pyrimidine moiety [29, 30]. In addition, different studies demonstrated the potent protein kinase inhibitory activity of some designed and synthesized pyrimidines. For instance, our group reported the VEGFR-2 inhibitory activity of a novel series of 2,4-disubstituted thiopyrimidines [27, 31].



Pazobanib (VI)



MKP116 (VII)

Fig. 3. The pyrimidine derivatives VI and VII as protein kinase inhibitors

Molecular hybridization is a recent and promising approach in medicinal chemistry that aims at linking two scaffolds to afford a new hybrid scaffold of improved activity [32]. Encouraged by the previous studies, our aim in this study is to design a new series of 5-nitrobenzimidazole-thiopyrimidine hybrids VIII as VEGFR-2 inhibitors (Fig. 4). Our design approach was tailored so that the benzimidazole moiety would fit in the gate area of the VEGFR-2 binding pocket stabilized through hydrogen bonding by its NH and C=N groups with the key amino acids Glu885 and Asp1046, respectively, whereas the methylenedioxy linker would act as a spacer extending the 2-thiopyrimidine moiety towards the hinge region (Fig. 4). The designed and synthesized benzimidazole-pyrimidine hybrids VIII were evaluated for their potential inhibitory activity of VEGFR-2. Simultaneously, the synthesized conjugates were screened for their cytotoxic activity on HepG2 cancer cell line. *In silico* molecular docking simulations were then carried out to predict the binding mode of the 5-nitrobenzimidazole-pyrimidine hybrids VIII within VEGFR-2 binding pocket. Moreover, prediction of the ADME properties of the synthesized

molecules was accomplished to study their predicted pharmacokinetic properties.

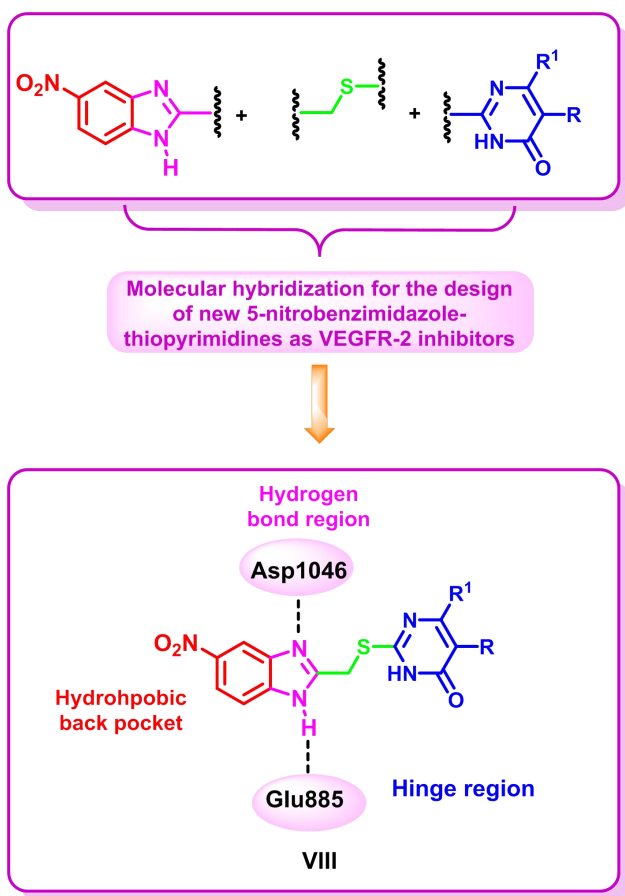


Fig. 4. Design of 5-nitrobenzimidazole-pyrimidine hybrids VIII as VEGFR-2 inhibitors

## 2. Experimental

### 2.1. Chemistry

#### 2.1.1. General remarks

Chemicals and solvents were purchased from commercial suppliers. Precoated silica gel 60 F<sub>245</sub> aluminium plates (Merck) were used to follow up the progress of the reactions. Melting points were recorded on a Stuart SMP30 melting point instrument. IR spectra were recorded on Jasco FT/IR 300E Fourier transform infrared spectrophotometer. <sup>1</sup>H NMR and <sup>13</sup>C NMR (DMSO-*d*<sub>6</sub>) spectra were measured at 400 and 100 MHz on Bruker instrument. Elemental analyses of the 5-nitrobenzimidazole derivatives were performed in the Microanalytical laboratory, Cairo University.

#### 2.1.2. Synthesis and analytical data of 12a,b, 13 and 14a-c

A mixture of the appropriate thiopyrimidine **3a,b**, **5** or **8a-c** (1 mmol), 2-(chloromethyl)-5-nitrobenzimidazole (**11**) (1 mmol) and anhydrous

potassium carbonate (1 mmol) were reacted under reflux for 2 hours. The mixture was then treated with water and few drops of 2*N* HCl. The precipitated product was filtered and purified by column chromatography using the eluent system (Petroleum ether/ Ethyl Acetate /MeOH 1:1:0.1).

#### • 2-(((5-Nitro-1*H*-benzo[*d*]imidazol-2-yl)methyl)thio)-6-propylpyrimidin-4(3*H*)-one (12a)

Yellowish brown powder; yield = 10%; mp 216-218 °C; IR (KBr)  $\tilde{\nu}$  3198, 3032, 2986, 2944, 1651, 1609, 1555, 1485, 1466 cm<sup>-1</sup>; <sup>1</sup>H NMR (400 MHz; DMSO-*d*<sub>6</sub>)  $\delta_{\text{H}}$  0.70 (3H, t, <sup>3</sup>*J* = 7.2 Hz), 1.42 (2H, q, <sup>3</sup>*J* = 7.2 Hz), 2.34 (2H, t, <sup>3</sup>*J* = 7.2 Hz), 4.76 (2H, s), 5.99 (1H, s), 7.66 (1H, d, <sup>3</sup>*J* = 8.8 Hz), 8.08 (1H, dd, <sup>3</sup>*J* = 8.8 Hz, <sup>4</sup>*J* = 2.0 Hz), 8.40 (1H, d, <sup>4</sup>*J* = 2.0 Hz), 12.61 ppm (1H, br.); Anal. Calcd for C<sub>15</sub>H<sub>15</sub>N<sub>5</sub>O<sub>3</sub>S: C, 52.16; H, 4.38; N, 20.28. Found: C, 52.39; H, 4.66; N, 20.40.

#### • 6-Isopropyl-2-(((5-nitro-1*H*-benzo[*d*]imidazol-2-yl)methyl)thio)pyrimidin-4(3*H*)-one (12b)

Yellowish brown powder; yield = 5%; mp 230-232 °C; IR (KBr)  $\tilde{\nu}$  3194, 3032, 2990, 2940, 2916, 1651, 1608, 1555, 1470 cm<sup>-1</sup>; <sup>1</sup>H NMR (400 MHz; DMSO-*d*<sub>6</sub>)  $\delta_{\text{H}}$  0.86 (6H, d, <sup>3</sup>*J* = 6.8 Hz), 2.94 (1H, septet, <sup>3</sup>*J* = 6.4 Hz), 4.90 (2H, s), 6.00 (1H, s), 7.59 (1H, d, <sup>3</sup>*J* = 7.6 Hz), 7.69 (1H, d, <sup>3</sup>*J* = 7.6 Hz), 8.09 (1H, s), 11.40 ppm (1H, s); Anal. Calcd for C<sub>15</sub>H<sub>15</sub>N<sub>5</sub>O<sub>3</sub>S: C, 52.16; H, 4.38; N, 20.28. Found: C, 52.42; H, 4.00; N, 20.49.

#### • 2-(((5-Nitro-1*H*-benzo[*d*]imidazol-2-yl)methyl)thio)-3,5,6,7-tetrahydro-4*H*-cyclopenta[*d*]pyrimidin-4-one (13)

Yellowish brown powder; yield = 12%; mp 254-256 °C; IR (KBr)  $\tilde{\nu}$  3198, 3028, 2990, 1651, 1605, 1555, 1470 cm<sup>-1</sup>; <sup>1</sup>H NMR (400 MHz; DMSO-*d*<sub>6</sub>)  $\delta_{\text{H}}$  1.93 (2H, pentet, <sup>3</sup>*J* = 7.2 Hz), 2.58 (2H, t, <sup>3</sup>*J* = 7.2 Hz), 2.72 (2H, t, <sup>3</sup>*J* = 7.2 Hz), 4.70 (2H, s), 7.67-7.69 (1H, m), 8.09 (1H, d, <sup>3</sup>*J* = 8.4 Hz), 8.42 (1H, s), 12.96 ppm (2H, br.); <sup>13</sup>C NMR (100 MHz; DMSO-*d*<sub>6</sub>)  $\delta_{\text{C}}$  20.68, 26.74, 27.42, 34.30, 117.84, 119.55, 142.67, 161.15, 161.26, 178.58 ppm; Anal. Calcd for C<sub>15</sub>H<sub>13</sub>N<sub>5</sub>O<sub>3</sub>S: C, 52.47; H, 3.82; N, 20.40. Found: C, 52.69; H, 3.57; N, 20.66.

#### • 2-(((5-Nitro-1*H*-benzo[*d*]imidazol-2-yl)methyl)thio)-6-oxo-4-phenyl-1,6-dihydropyrimidine-5-carbonitrile (14a)

Yellow powder; yield = 20%; mp 262-264 °C;  $\delta_{\text{H}}$  (400 MHz; DMSO-*d*<sub>6</sub>) 4.95 (2H, s), 6.86-6.87 (1H, m), 7.10-7.11 (2H, m), 7.49-7.53 (2H, m), 7.64-7.67 (1H, m), 8.01-8.03 ppm (2H, m); Anal. Calcd for C<sub>19</sub>H<sub>12</sub>N<sub>6</sub>O<sub>3</sub>S: C, 56.43; H, 2.99; N, 20.78. Found: C, 56.67; H, 3.24; N, 20.54.

**• 2-(((5-Nitro-1*H*-benzo[*d*]imidazol-2-yl)methyl)thio)-6-oxo-4-(*p*-tolyl)-1,6-dihydropyrimidine-5-carbonitrile (14b)**

Yellow powder; yield = 25%; mp 233-235 °C; <sup>1</sup>H-NMR (400 MHz; DMSO-*d*<sub>6</sub>) δ<sub>H</sub> 2.34 (3H, s), 4.63 (2H, s), 7.25 (2H, d, <sup>3</sup>*J* = 8.0 Hz), 7.65-7.68 (3H, m), 8.07 (1H, dd, <sup>3</sup>*J* = 8.9 Hz, <sup>4</sup>*J* = 2.2 Hz), 8.42 ppm (1H, d, <sup>4</sup>*J* = 2.2 Hz); <sup>13</sup>C-NMR (100 MHz; DMSO-*d*<sub>6</sub>) δ<sub>C</sub> 21.04, 27.79, 89.86, 117.71, 118.91, 128.35, 128.87, 133.97, 140.43, 142.54, 157.11, 167.31, 169.40 ppm; Anal. Calcd for C<sub>20</sub>H<sub>14</sub>N<sub>6</sub>O<sub>3</sub>S: C, 57.41; H, 3.37; N, 20.09. Found: C, 57.22; H, 3.58; N, 20.35.

**• 4-(4-Methoxyphenyl)-2-(((5-nitro-1*H*-benzo[*d*]imidazol-2-yl)methyl)thio)-6-oxo-1,6-dihydropyrimidine-5-carbonitrile (14c)**

Yellow powder; yield = 21%; mp 236-238 °C; <sup>1</sup>H-NMR (400 MHz; DMSO-*d*<sub>6</sub>) δ<sub>H</sub> 3.73 (3H, s), 4.91 (2H, s), 7.01 (2H, d, <sup>3</sup>*J* = 8.0 Hz), 7.12 (2H, d, <sup>3</sup>*J* = 8.5 Hz), 7.46 (1H, d, <sup>3</sup>*J* = 8.0 Hz), 8.09-8.11 ppm (2H, m); Anal. Calcd for C<sub>20</sub>H<sub>14</sub>N<sub>6</sub>O<sub>4</sub>S: C, 55.30; H, 3.25; N, 19.35. Found: 55.00; H, 3.47; N, 19.04.

## 2.2. Biology

### 2.2.1. Screening of the inhibitory activity of the 5-nitrobenzimidazole-pyrimidine hybrids 12a,b, 13 and 14a-c on VEGFR-2

The synthesized benzimidazole-pyrimidine hybrids **12a,b**, **13** and **14a-c** were screened for their ability to suppress the activity of VEGFR-2 and their IC<sub>50</sub> values were calculated using VEGFR-2 kinase kit (BPS Biosciences - San Diego - CA - US) according to the manufacturer procedure.

### 2.2.2. *In vitro* anticancer screening on HepG2 cell line.

The synthesized 5-nitrobenzimidazole-pyrimidine hybrids **12a,b**, **13**, **14a-c** were assayed in National Cancer Institute, Egypt for their cytotoxic activity on HepG2 cell line according to the reported procedure and their IC<sub>50</sub> values were calculated [33].

## 2.3. *In silico* studies

### 2.3.1. Molecular Modeling

Docking studies were performed by molecular operating environment software (MOE, 2020.0901) according to the reported method [27, 31].

### 2.3.2. Prediction of ADME properties

ADME properties were predicted from SwissADME free webtool [34-38].

## 3. Results and discussion

### 3.1. Chemistry

For the synthesis of the target 5-nitrobenzimidazole-thiopyrimidine conjugates **12a,b**, **13** and **14a-c**, the intermediates **3a,b**, **5** as well as **8a-c** were initially synthesized according to the previously

reported procedures as shown in scheme 1 [24, 31, 39-41]. Concurrently, 2-(chloromethyl)-5-nitro-1*H*-benzo[*d*]imidazole (**11**) was synthesized by the reaction of 4-nitro-*o*-phenylenediamine (**9**) and chloroacetic acid (**10**) in 4*N* HCl. Subsequently, the 2-chloromethyl benzimidazole derivative **11** was reacted with the thiopyrimidine derivatives **3a,b**, **5** and **8** under basic conditions to afford the corresponding target compounds **12a,b**, **13** and **14a-c**, respectively (Scheme 1).

## 3.2. Biological Evaluation

### 3.2.1. VEGFR-2 kinase inhibitory activity.

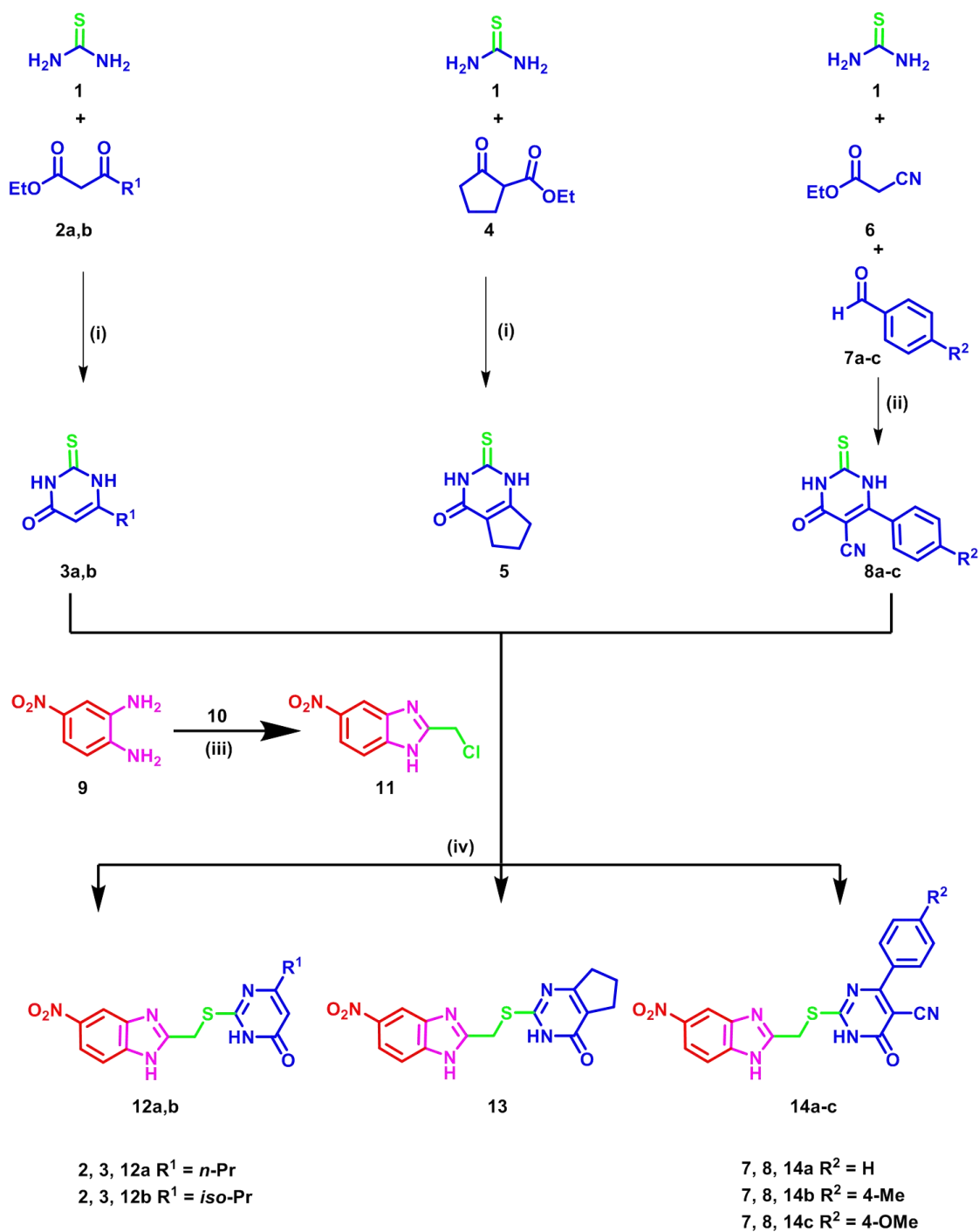
The synthesized 5-nitrobenzimidazole-pyrimidine hybrids **12a,b**, **13** and **14a-c** were evaluated for their inhibitory activity against VEGFR-2. The IC<sub>50</sub> (μM) of the synthesized derivatives as well as sorafenib (**I**) were depicted in Table 1. The recorded results revealed that series **14a-c** showed a significantly more potent inhibitory activity than that of series **12a,b** and **13**.

In series **12a,b**, the substituent at the 4-position of the pyrimidine moiety affects the activity, compound **12a** exhibiting *n*-propyl group showed very weak VEGFR-2 inhibitory activity with IC<sub>50</sub> = 32.96 μM, whereas the isopropyl congener **12b** displayed approximately two-fold increase in the potency with IC<sub>50</sub> of 16.91 μM. Replacing the pyrimidine moiety in series **12a,b** with cyclopentyl thiopyrimidine in **13** showed weak inhibitory activity on VEGFR-2 with IC<sub>50</sub> of 28.94 μM. A great increase in the potency was observed in series **14a-c** where the aliphatic groups in **12a,b** were replaced with aromatic substituents, beside the incorporation of a carbonitrile group at position 5. Compound **14c** is the most potent compound of the synthesized series with IC<sub>50</sub> of 2.83 μM, whereas the 4-methylphenyl derivative **14b** demonstrated less potency with IC<sub>50</sub> of 3.68 μM and the unsubstituted phenyl derivatives **14a** (IC<sub>50</sub> = 7.01 μM) showed more than two-fold less potency in comparison to **14c** (IC<sub>50</sub> = 2.83 μM).

**Table 1.** Biochemical inhibitory activity of the synthesized 5-nitrobenzimidazole-pyrimidine conjugates **12a,b**, **13**, and **14a-c** on VEGFR-2

Compound	VEGFR-2
	IC <sub>50</sub> (μM) <sup>a</sup>
<b>12a</b>	32.96 ± 2.53
<b>12b</b>	16.91 ± 0.89
<b>13</b>	28.94 ± 2.10
<b>14a</b>	7.01 ± 0.56
<b>14b</b>	3.68 ± 0.19
<b>14c</b>	2.83 ± 0.15
Sorafenib ( <b>I</b> )	0.10 ± 0.01

<sup>a</sup>Mean of two different experiments



Reaction conditions: (i) KOH, EtOH, reflux, 7h; (ii) anhydrous K<sub>2</sub>CO<sub>3</sub>, EtOH, reflux, 7h; (iii) ClCH<sub>2</sub>COOH (10), 4N HCl, reflux, 6h; (iv) anhydrous K<sub>2</sub>CO<sub>3</sub>, EtOH, reflux, 2h.

Scheme 1. Synthesis of benzimidazole-pyrimidine hybrids 12a,b, 13, 14a-c

### 3.2.2. *In vitro* anti-proliferative activity

Sulfo-Rhodamine-B (SRB) assay was employed for *in vitro* screening of the designed and synthesized 5-nitrobenzimidazole-thiopyrimidine conjugates **12a,b**, **13**, **14a-c** in comparison to sorafenib (**I**) for their cytotoxic activity on HepG2 cell line [33]. The obtained IC<sub>50</sub> values were presented in table 2. The synthesized derivatives displayed potent to moderate IC<sub>50</sub> values on HepG2 cell lines with IC<sub>50</sub> of 4.37 to 57.46 μM in comparison to sorafenib (**I**) (IC<sub>50</sub> = 3.34 μM). Compound **14c** is the most potent compound in the synthesized series, it displayed IC<sub>50</sub> = 4.37 μM. In series **12a,b**, compound **12a** with *n*-propyl substituent showed moderate inhibitory activity on HepG2 cell line with IC<sub>50</sub> = 43.42 μM. Replacement of *n*-propyl group in **12a** with isopropyl moiety in **12b** showed more than two-fold increase in potency with IC<sub>50</sub> = 18.37 μM. Replacement of substituted thiouracil in **12a,b** with cyclopentyl thiouracil in **13** showed a decrease in the activity (IC<sub>50</sub> = 57.46 μM). Meanwhile, replacement of 4-aliphatic substituted thiouracils in **12a,b** with phenyl substituted thiouracil and introduction of a carbonitrile group in the 5 position in **14a-c** resulted in increasing in potency (IC<sub>50</sub> = 4.37 to 23.65 μM). In series **14a-c**, the phenyl derivative showed a moderate activity with IC<sub>50</sub> of 23.65 μM, whereas the introduction of a 4-methylphenyl group in **14b** or 4-methoxyphenyl group in **14c** resulted in increasing in potency with IC<sub>50</sub> of 13.92 and 4.37 μM, respectively.

**Table 2.** Cytotoxic activity of the synthesized benzimidazole-pyrimidine conjugates **12a,b**, **13**, **14a-c** on HepG2 cell line

Compound	IC <sub>50</sub> (μM)
<b>12a</b>	43.42 ± 2.10
<b>12b</b>	18.37 ± 1.30
<b>13</b>	57.46 ± 3.60
<b>14a</b>	23.65 ± 1.10
<b>14b</b>	13.92 ± 0.92
<b>14c</b>	4.37 ± 0.25
<b>Sorafenib (I)</b>	3.34 ± 0.200

### 3.3. Molecular docking studies

Molecular docking of the synthesized benzimidazole-pyrimidine hybrids **12a,b**, **13** and **14a-c** in the binding pocket of VEGFR-2 was conducted to study the binding interaction of the synthesized molecules with the key amino acids. Molecular Operating Environment (MOE, 2020.0901) software was used. The X-ray crystal structure of VEGFR-2 (co-crystallized with sorafenib (**I**)) (PDB ID: 4ASD) was downloaded from the Protein Data Bank [42]. The previously prepared and validated docking protocol was employed for the current

molecular docking simulation and the resulted binding energy scores were presented in table 3 [31]. The synthesized derivatives demonstrated energy scores (*S*) of -11.88 to -15.13 kcal/mol compared to sorafenib (**I**) (*S* = -15.19 kcal/mol) (Table 3).

**Table 3.** Docking energy scores (*S*) in kcal/mol of the 5-nitrobenzimidazole-pyrimidine conjugates **12a,b**, **13**, **14a-c** and sorafenib (**I**) in VEGFR-2 active site.

Compound	Energy score ( <i>S</i> ) kcal/mol
<b>12a</b>	-12.47
<b>12b</b>	-12.33
<b>13</b>	-11.88
<b>14a</b>	-13.96
<b>14b</b>	-15.13
<b>14c</b>	-14.94
<b>Sorafenib</b>	-15.19

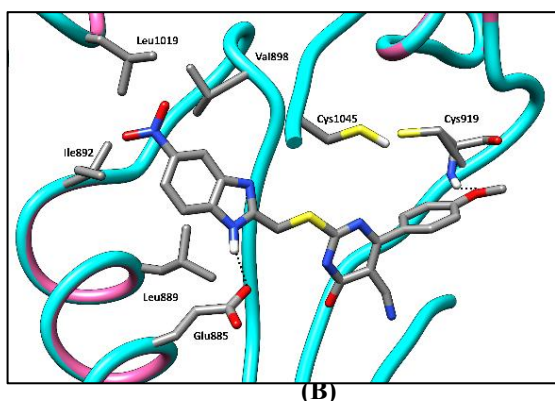
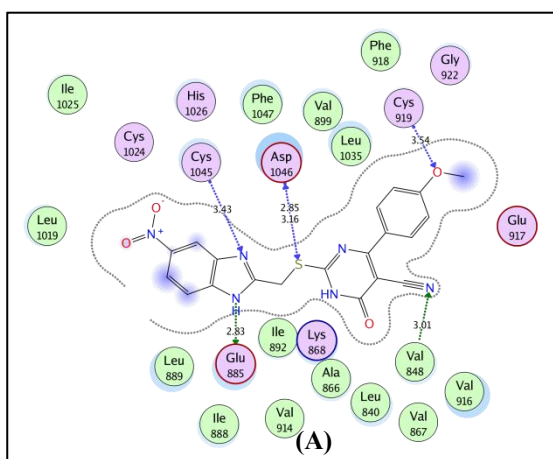
The synthesized derivatives revealed a similar general binding mode in the binding pocket of VEGFR-2. The benzimidazole moiety occupies the gate area where the imidazole moiety is involved in hydrogen bonding interaction through its NH and C=N groups with the key amino acids Glu885 and Cys1045, respectively. The methylenethio spacer interacts with the key amino acid Asp1046. The thiopyrimidine moiety is directed towards the hinge region where it is involved in hydrophobic interaction with Leu840, Val848, Val899, Phe918, Cys919, Leu1015, Leu1035, and Phe1047 amino acids. In compounds **14b** and **14c**, the thiopyrimidine moiety performs through the carbonitrile moiety in **14b** or 4-methoxyphenyl group in **14c** hydrogen bonding with hinge region Cys919. The fused benzene ring of the benzimidazole moiety is oriented towards the hydrophobic back pocket and is involved in hydrophobic interactions with Ile888, Leu889, Ile892, Val898, Val899, Leu1019, and Ile1044 amino acids (Fig. 5) (2D for the rest of derivatives were depicted in SI)

### 3.4. *In silico* prediction of physicochemical, pharmacokinetic and ADME properties of 5-nitro-benzimidazole derivatives **12a,b**, **13**, **14a-c**

Prediction of the ADME properties of the designed and synthesized benzimidazole-pyrimidine conjugates **12a,b**, **13** and **14a-c** was done using SwissADME webtool [34]. Representative examples are depicted in table 4. As can be noticed the hybrids **12a,b**, **13**, **14a-c**, displayed acceptable physicochemical properties including acceptable molecular weights, *logP* (octanol-water partition coefficient) [37] and topological polar surface area (TPSA).

**Table 4.** Physicochemical properties of the synthesized 5-nitrobenzimidazole-pyrimidine hybrids **12a,b, 13, 14a-c**

Compound ID	MW	#Rotatable e bonds	#H-bond acceptors	#H-bond donors	MR	TPSA	iLOGP	BBB permeant	Pgp substrate	Lipinski #violations	Bioavailability Score
<b>12a</b>	345.38	6	5	2	94.12	145.55	1.82	No	No	0	0.55
<b>12b</b>	345.38	5	5	2	94.12	145.55	1.71	No	No	0	0.55
<b>13</b>	343.36	4	5	2	92.16	145.55	1.82	No	Yes	0	0.55
<b>14a</b>	404.4	5	6	2	109.69	169.34	1.09	No	No	0	0.55
<b>14b</b>	418.43	5	6	2	114.66	169.34	1.31	No	No	0	0.55
<b>14c</b>	434.43	6	7	2	116.18	178.57	1.85	No	No	0	0.55

**Fig. 5.** 2D diagram (A) and 3D representation (B) showing interactions of compound **14c** in VEGFR-2 binding pocket

The synthesized conjugates are predicated to be well absorbed from GIT with no BBB permeability. Meanwhile, most of them are not substrate for P-glycoprotein (P-gp) the key transporter that is responsible for eliminating foreign substances from the cells [43]. In addition, all the synthesized hybrids do not violate Lipinski's rule of 5 and revealed promising bioavailability score. In addition, they do not include any of the Pan Assay Interference (PAINS) fragments [38].

#### 4. Conclusion

A new series of 5-nitrobenzimidazole-pyrimidine hybrids **12a,b, 13, and 14a-c** were designed and synthesized as VEGFR-2 inhibitors. The conjugates revealed moderate to potent VEGFR-2 inhibitory activity. Compounds **14b** and **14c** demonstrated  $IC_{50}$  of 3.68 and 2.83  $\mu$ M, respectively. In addition, the synthesized conjugates exhibited cytotoxic activity on the HepG2 cell line. Likewise, compounds **14b** and **14c** were the most potent derivatives with  $IC_{50}$  of 13.92 and 4.37  $\mu$ M, respectively. Molecular docking simulations of the synthesized hybrids in VEGFR-2 binding site demonstrated that the benzimidazole moiety occupies the gate area forming hydrogen bonding interactions through its NH and C=N groups with Glu885 and Cys1045, respectively. The methylenethio spacer interacts with the key residue Asp1046. The thiouracil moiety is oriented towards the hinge region and is involved in hydrogen bonding and hydrophobic interactions with the amino acids surrounding this region. The benzimidazole benzene ring is oriented towards the hydrophobic back pocket and is involved in hydrophobic interactions. In addition, the synthesized conjugates exhibit satisfactory physicochemical properties that can be slightly optimized for the discovery of novel anti-angiogenic and anticancer agents.

#### 5. Conflicts of interest

There are no conflicts to declare.

#### 6. References

- [1] H. Rumgay, M. Arnold, J. Ferlay, O. Lesi, C.J. Cabasag, J. Vignat, M. Laversanne, K.A. McGlynn, I. Soerjomataram, Global burden of primary liver cancer in 2020 and predictions to 2040, *J Hepatol*, 77, 1598-1606 (2022).
- [2] M.A. Morse, W. Sun, R. Kim, A.R. He, P.B. Abada, M. Mynderse, R.S. Finn, The Role of

- Angiogenesis in Hepatocellular Carcinoma, *Clin Cancer Res*, 25, 912-920 (2019).
- [3] C. Yao, S. Wu, J. Kong, Y. Sun, Y. Bai, R. Zhu, Z. Li, W. Sun, L. Zheng, Angiogenesis in hepatocellular carcinoma: mechanisms and anti-angiogenic therapies, *Cancer Biology & Medicine*, 20, 25-43 (2023).
- [4] C. Yao, S. Wu, J. Kong, Y. Sun, Y. Bai, R. Zhu, Z. Li, W. Sun, L. Zheng, Angiogenesis in hepatocellular carcinoma: mechanisms and anti-angiogenic therapies, *Cancer Biol Med*, 20, 25-43 (2023).
- [5] A.W. Griffioen, Angiogenesis, in: M. Schwab (Ed.) *Encyclopedia of Cancer*, Springer Berlin Heidelberg, Berlin, Heidelberg, 2011, pp. 185-186.
- [6] J. Folkman, Tumor angiogenesis: therapeutic implications, *N Engl J Med*, 285, 1182-1186 (1971).
- [7] Z.-L. Liu, H.-H. Chen, L.-L. Zheng, L.-P. Sun, L. Shi, Angiogenic signaling pathways and anti-angiogenic therapy for cancer, *Signal Transduction and Targeted Therapy*, 8, 198 (2023).
- [8] J. Folkman, Angiogenesis: an organizing principle for drug discovery?, *Nat Rev Drug Discov*, 6, 273-286 (2007).
- [9] M. Berretta, L. Rinaldi, F. Di Benedetto, A. Lleshi, V. De Re, G. Facchini, P. De Paoli, R. Di Francia, Angiogenesis inhibitors for the treatment of hepatocellular carcinoma, *Front Pharmacol*, 7, 428 (2016).
- [10] J.M. Llovet, S. Ricci, V. Mazzaferro, P. Hilgard, E. Gane, J.F. Blanc, A.C. de Oliveira, A. Santoro, J.L. Raoul, A. Forner, M. Schwartz, C. Porta, S. Zeuzem, L. Bolondi, T.F. Greten, P.R. Galle, J.F. Seitz, I. Borbath, D. Haussinger, T. Giannaris, M. Shan, M. Moscovici, D. Voliotis, J. Bruix, S.I.S. Group, Sorafenib in advanced hepatocellular carcinoma, *N Engl J Med*, 359, 378-390 (2008).
- [11] B. Xie, D.H. Wang, S.J. Spechler, Sorafenib for treatment of hepatocellular carcinoma: a systematic review, *Dig Dis Sci*, 57, 1122-1129 (2012).
- [12] Y.J. Zhu, B. Zheng, H.Y. Wang, L. Chen, New knowledge of the mechanisms of sorafenib resistance in liver cancer, *Acta Pharmacol Sin*, 38, 614-622 (2017).
- [13] Z. Jiang, C. Dai, Potential Treatment Strategies for Hepatocellular Carcinoma Cell Sensitization to Sorafenib, *J Hepatocell Carcinoma*, 10, 257-266 (2023).
- [14] J. Bruix, S. Qin, P. Merle, A. Granito, Y.H. Huang, G. Bodoky, M. Pracht, O. Yokosuka, O. Rosmorduc, V. Breder, R. Gerolami, G. Masi, P.J. Ross, T. Song, J.P. Bronowicki, I. Ollivier-Hourmand, M. Kudo, A.L. Cheng, J.M. Llovet, R.S. Finn, M.A. LeBerre, A. Baumhauer, G. Meinhardt, G. Han, R. Investigators, Regorafenib for patients with hepatocellular carcinoma who progressed on sorafenib treatment (RESORCE): a randomised, double-blind, placebo-controlled, phase 3 trial, *Lancet*, 389, 56-66 (2017).
- [15] M. Kudo, R.S. Finn, S. Qin, K.H. Han, K. Ikeda, F. Piscaglia, A. Baron, J.W. Park, G. Han, J. Jassem, J.F. Blanc, A. Vogel, D. Komov, T.R.J. Evans, C. Lopez, C. Dutcus, M. Guo, K. Saito, S. Kraljevic, T. Tamai, M. Ren, A.L. Cheng, Lenvatinib versus sorafenib in first-line treatment of patients with unresectable hepatocellular carcinoma: a randomised phase 3 non-inferiority trial, *Lancet*, 391, 1163-1173 (2018).
- [16] J. Gile, M.E. Palmer, M.H. Storandt, T.S. Bekaii-Saab, N.H. Tran, A. Mahipal, Outcome of receiving lenvatinib following immunotherapy in patients with advanced hepatocellular carcinoma, *Journal of Clinical Oncology*, 41, 507-507 (2023).
- [17] Y.T. Lee, Y.J. Tan, C.E. Oon, Benzimidazole and its derivatives as cancer therapeutics: The potential role from traditional to precision medicine, *Acta Pharm Sin B*, 13, 478-497 (2023).
- [18] H.T. Abdel-Mohsen, F.A. Ragab, M.M. Ramla, H.I. El Diwani, Novel benzimidazole-pyrimidine conjugates as potent antitumor agents, *Eur J Med Chem*, 45, 2336-2344 (2010).
- [19] H.I. El Diwani, H.T. Abdel-Mohsen, I. Salama, F.A.-F. Ragab, M.M. Ramla, S.A. Galal, M.M. Abdalla, A. Abdel-Wahab, M.A. El Demellawy, Synthesis, Molecular Modeling, and Biological Evaluation of Novel Benzimidazole Derivatives as Inhibitors of Hepatitis C Virus RNA Replication, *Chemical and Pharmaceutical Bulletin*, 62, 856-866 (2014).
- [20] I.H. Ali, H.T. Abdel-Mohsen, M.M. Mounier, M.T. Abo-Elfadl, A.M. El Kerdawy, I.A.Y. Ghannam, Design, synthesis and anticancer activity of novel 2-arylbenzimidazole/2-thiopyrimidines and 2-thioquinazolin-4(3H)-ones conjugates as targeted RAF and VEGFR-2 kinases inhibitors, *Bioorg Chem*, 126, 105883 (2022).
- [21] M.A. Abdullaziz, H.T. Abdel-Mohsen, A.M. El Kerdawy, F.A.F. Ragab, M.M. Ali, S.M. Abu-Bakr, A.S. Girgis, H.I. El Diwani, Design, synthesis, molecular docking and cytotoxic evaluation of novel 2-furybenzimidazoles as VEGFR-2 inhibitors, *Eur J Med Chem*, 136, 315-329 (2017).

- [22] H.T. Abdel-Mohsen, M.A. Abdullaziz, A.M.E. Kerdawy, F.A.F. Ragab, K.J. Flanagan, A.E.E. Mahmoud, M.M. Ali, H.I.E. Diwani, M.O. Senge, Targeting Receptor Tyrosine Kinase VEGFR-2 in Hepatocellular Cancer: Rational Design, Synthesis and Biological Evaluation of 1,2-Disubstituted Benzimidazoles, *Molecules*, 25, 770 (2020).
- [23] A. Mahapatra, T. Prasad, T. Sharma, Pyrimidine: a review on anticancer activity with key emphasis on SAR, *Future Journal of Pharmaceutical Sciences*, 7, 123 (2021).
- [24] H.T. Abdel-Mohsen, A. Petreni, C.T. Supuran, Investigation of the carbonic anhydrase inhibitory activity of benzenesulfonamides incorporating substituted fused-pyrimidine tails, *Arch Pharm (Weinheim)*, 355, e2200274 (2022).
- [25] S.S. Abd El-Karim, Y.M. Syam, A.M. El Kerdawy, H.T. Abdel-Mohsen, Rational design and synthesis of novel quinazolinone N-acetohydrazides as type II multi-kinase inhibitors and potential anticancer agents, *Bioorganic Chemistry*, 142, 106920 (2024).
- [26] H.T. Abdel-Mohsen, A.M. El Kerdawy, M.A. Omar, E. Berrino, A.S. Abdelsamie, H.I. El Diwani, C.T. Supuran, New thiopyrimidine-benzenesulfonamide conjugates as selective carbonic anhydrase II inhibitors: synthesis, in vitro biological evaluation, and molecular docking studies, *Bioorganic & Medicinal Chemistry*, 28, 115329 (2020).
- [27] H.T. Abdel-Mohsen, A.S. Girgis, A.E.E. Mahmoud, M.M. Ali, H.I. El Diwani, New 2,4-disubstituted-2-thiopyrimidines as VEGFR-2 inhibitors: Design, synthesis, and biological evaluation, *Arch Pharm (Weinheim)*, 352, e1900089 (2019).
- [28] H.T. Abdel-Mohsen, M.A. Omar, O. Kutkat, A.M.E. Kerdawy, A.A. Osman, M. GabAllah, A. Mostafa, M.A. Ali, H.I.E. Diwani, Discovery of novel thioquinazoline-N-aryl-acetamide/N-arylacetohydrazide hybrids as anti-SARS-CoV-2 agents: Synthesis, in vitro biological evaluation, and molecular docking studies, *Journal of Molecular Structure*, 1276, 134690 (2023).
- [29] D.T. Nguyen, S. Shayahi, Pazopanib: approval for soft-tissue sarcoma, *J Adv Pract Oncol*, 4, 53-57 (2013).
- [30] R. Dagher, M. Cohen, G. Williams, M. Rothmann, J. Gobburu, G. Robbie, A. Rahman, G. Chen, A. Staten, D. Griebel, R. Pazdur, Approval summary: imatinib mesylate in the treatment of metastatic and/or unresectable malignant gastrointestinal stromal tumors, *Clin Cancer Res*, 8, 3034-3038 (2002).
- [31] H.T. Abdel-Mohsen, M.A. Omar, A.M. El Kerdawy, A.E.E. Mahmoud, M.M. Ali, H.I. El Diwani, Novel potent substituted 4-amino-2-thiopyrimidines as dual VEGFR-2 and BRAF kinase inhibitors, *Eur J Med Chem*, 179, 707-722 (2019).
- [32] G. Berube, An overview of molecular hybrids in drug discovery, *Expert Opin Drug Discov*, 11, 281-305 (2016).
- [33] P. Skehan, R. Storeng, D. Scudiero, A. Monks, J. McMahon, D. Vistica, J.T. Warren, H. Bokesch, S. Kenney, M.R. Boyd, New colorimetric cytotoxicity assay for anticancer-drug screening, *J Natl Cancer Inst*, 82, 1107-1112 (1990).
- [34] A. Daina, O. Michielin, V. Zoete, SwissADME: a free web tool to evaluate pharmacokinetics, drug-likeness and medicinal chemistry friendliness of small molecules, *Sci Rep*, 7, 42717 (2017).
- [35] H.T. Abdel-Mohsen, A. Abood, K.J. Flanagan, A. Meindl, M.O. Senge, H.I. El Diwani, Synthesis, crystal structure, and ADME prediction studies of novel imidazopyrimidines as antibacterial and cytotoxic agents, *Arch Pharm (Weinheim)*, 353, e1900271 (2020).
- [36] H.T. Abdel-Mohsen, E.A. Abd El-Meguid, A.M. El Kerdawy, A.E.E. Mahmoud, M.M. Ali, Design, synthesis, and molecular docking of novel 2-arylbenzothiazole multiangiokinase inhibitors targeting breast cancer, *Arch Pharm (Weinheim)*, 353, e1900340 (2020).
- [37] A. Daina, O. Michielin, V. Zoete, iLOGP: a simple, robust, and efficient description of n-octanol/water partition coefficient for drug design using the GB/SA approach, *J Chem Inf Model*, 54, 3284-3301 (2014).
- [38] J.B. Baell, G.A. Holloway, New substructure filters for removal of pan assay interference compounds (PAINS) from screening libraries and for their exclusion in bioassays, *J Med Chem*, 53, 2719-2740 (2010).
- [39] H.T. Abdel-Mohsen, A.M. El Kerdawy, M.A. Omar, A. Petreni, R.M. Allam, H.I. El Diwani, C.T. Supuran, Application of the dual-tail approach for the design and synthesis of novel Thiopyrimidine-Benzenesulfonamide hybrids as selective carbonic anhydrase inhibitors, *Eur J Med Chem*, 228, 114004 (2022).
- [40] H.T. Abdel-Mohsen, A.M. El Kerdawy, A. Petreni, C.T. Supuran, Novel benzenesulfonamide-thiouracil conjugates with a flexible N-ethyl acetamide linker as selective CA IX and CA XII inhibitors, *Arch Pharm (Weinheim)*, 356, e2200434 (2023).
- [41] H.T. Abdel-Mohsen, J. Conrad, K. Harms, D. Nohr, U. Beifuss, Laccase-catalyzed green

- synthesis and cytotoxic activity of novel pyrimidobenzothiazoles and catechol thioethers, *RSC Advances*, 7, 17427-17441 (2017).
- [42] M. McTigue, B.W. Murray, J.H. Chen, Y.L. Deng, J. Solowiej, R.S. Kania, Molecular conformations, interactions, and properties associated with drug efficiency and clinical performance among VEGFR TK inhibitors, *Proc Natl Acad Sci U S A*, 109, 18281-18289 (2012).
- [43] M.L. Amin, P-glycoprotein Inhibition for Optimal Drug Delivery, *Drug Target Insights*, 7, 27-34 (2013).